

Theoretical model to determine bond loss in prestressed concrete with reinforcement corrosion

Néstor F. Ortega^{*1,2}, Juan M. Moro^{1,3a} and Romina S. Meneses^{1b}

¹Engineering Institute, Engineering Department, Universidad Nacional del Sur, Av. Alem 1254, (8000) Bahía Blanca, Argentina

²Comisión de Investigaciones Científicas de la Provincia de Buenos Aires, Argentina

³Consejo Nacional de Investigaciones Científicas y Tecnológicas, (C1033AAJ) CABA, Argentina

(Received February 22, 2017, Revised November 29, 2017, Accepted November 30, 2017)

Abstract. This paper reviews the mechanical effects produced by reinforcement corrosion of prestressed concrete beams. Specifically, modifications in the bonding of the tendon to the concrete that reduce service life and load bearing capacity are studied. Experimental information gathered from previous works has been used for the theoretical analysis. Relationships between bond stress loss and reinforcement penetration in the concrete, and concrete external cracking were established. Also, it was analysed the influence that has the location of the area affected by corrosion on the loss magnitude of the initial prestress.

Keywords: corrosion; prestressed concrete; bond; cracking

1. Introduction

Over time and due to different factors, concrete structures suffer a degradation process originated from concrete carbonation, chlorine penetration and alkali-aggregate reaction, among others. The first cause of the pH decrease at the interface area between the steel and the concrete, this causes the activation of the corrosion process. These oxides occupy a bigger volume than the affected steel, filling the concrete pore structure and pressing the concrete near the bars, until the breaking point of the concrete is reached and the cover cracks. These cracks represent an entrance for the external agents that favour reinforcement corrosion, which accelerates the degradation process and decreases the service life of the damaged structure.

In the corrosion processes of reinforced concrete structures, there are different parameters that characterize the kinetics of this degradation process. The main parameters are: the quality of cover concrete (Cabrera *et al.* 2012), the thickness of cover (cover/diameter of the affected reinforcements ratio) (Ortega *et al.* 2011, Meneses *et al.* 2016) and the tensional state of reinforcements and cover concrete (Aveldaño and Ortega 2013). These parameters are in direct relation with corrosion process speed of the reinforcements, which is evidenced by the current intensity and the cover cracks generated in the affected structure.

Mechanical effects of the damaged concrete elements due to corrosion of the metallic reinforcements, in particular prestressed ones, are studied. In prestressed structures, the

stress applied to the reinforcements, without the use of the traditional ties in post-tensioned structures, is transmitted to the concrete by bonding. This is an interesting research point since there are a great number of structures with prestressed reinforcements, mostly precast ones. It is important to remember that these reinforcements are subjected to tensile stresses that accelerate the corrosion rate. This process is known as “stress corrosion”,

Reinforcement corrosion produces three damaging different effects on concrete structures that diminish the effective Inertia of the resistant cross-section, altering the static and dynamic behaviour of the affected element. These related effects are:

a. Concrete cracking (mostly on the cover area), due to tensile stresses originated by the appearance of corrosion products which present a larger volume than the affected material (Jin *et al.* 2015, Aimin *et al.* 2016, Gerengiet *et al.* 2017) causes a decrease of the concrete useful section.

b. Reduction of the cross-section of the affected reinforcements, which can lead to their breaking point when the maximum tensile strength is reached (Castaldo *et al.* 2017, Gerengi *et al.* 2017), and

c. Bond loss between concrete and steel, due to the corrosion process at the interface area and the confinement loss as consequence of the cover cracking, (Chung *et al.* 2004, Yalciner *et al.* 2012, Sajedi *et al.* 2015).

Other research works have studied, from a physical and an electrochemical point of view, steel-concrete interface properties of corroded reinforcements (Liu *et al.* 2016, Lollini *et al.* 2016). Also, numerical models have been developed, to predict the cracking of the concrete cover, originated by reinforcement corrosion (Hosseini *et al.* 2015, Zhao *et al.* 2016).

It is worth to mention that in all previously mentioned references, the corrosion process is analysed on reinforced concrete structures (Yuksel 2015). Regarding corrosion of prestressed concrete elements has been barely studied in

*Corresponding author, Full Professor

E-mail: nfortega@criba.edu.ar

^aPh.D.

^bPh.D. Student

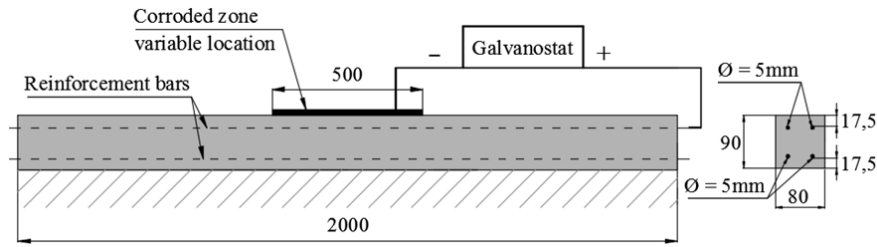


Fig. 1 Schematic model of tested beams (dimensions in mm)

laboratories; some references about this topic can be found in References (Permanent Committee of the Concrete 1998, Leonhart 1988).

This research from an analytical point of view is based on the experimental work made at the Institute of Building Sciences “E. Torroja” (Ortega *et al.* 2001a).

From these experimental research and a series of recommendations and equations that are mentioned at References (Permanent Committee of the Concrete 1998; Euro-International Committee of Concrete 1990, UNE 7-436-82 1993, LCPC 1999), the bond loss due to reinforcement corrosion for the different studied cases was determined.

2. Materials and methodology

2.1 Characteristics of the studied beams

Test specimens (beams) where reinforcement bond was studied, were moulded according to the test method to determine bond reinforcement characteristics (Spanish norm UNE 7-436-82 1993), with the following characteristic:

- Section: 80×90 mm
- Length: 2000 mm
- Average concrete stress: 25 N mm⁻²
- Cement: Type I 42.5 R (High Initial Strength)
- Cement content: 300 concrete kg m⁻³
- A/C ratio=0.53
- Complete Reinforcement: 4 reinforcement bars, diameter: 5 mm (2 upper bars and 2 lower bars)
- Steel Elasticity Modulus: 215800 N mm⁻²
- Breaking effort of each bar: 37.3 kN
- Stressed effort of each bar: 29.4 kN
- Concrete cover: 17.5 mm

2.2 Bond test

Reinforcements were anchored to a prestressing bench, to apply the tensile strength to each bar. After 24hs approximately, and once the losses generated by anchorage sinking and steel relaxation were verified ($\leq 3\%$), the concrete was placed in the formworks.

After the molding stage, test specimens were cured in their formworks with a high percentage of moisture. Once the formwork was removed, during the first week, the test specimens were kept in a moist atmosphere. Then, during 21 days, they were left in the prestressing bench, exposed to



Fig. 2 Beam IV during the accelerated corrosion process

laboratory conditions (environmental temperature $\cong 20^\circ\text{C}$ and HR $\cong 50\%$), until tendons were loosened from their anchoring and prestressed forces begin to appear in the beams. Before this, cylindrical test specimens of 15×30 cm were tested to verify the concrete strength.

When concrete reaches the desired strength, tendons are loosened from its anchorages. From that moment and for a minimum term of 7 days, penetration at the end of each tendon is measured. Also, longitudinal strains of the beams are registered. This test type is known as “push in”,

2.3 Accelerated corrosion process

The beams were supported in all their length during the entire test, to lessen the influence of tensions on the reinforcements by dead loads. In Corrosion tests was applied a constant current density of 200 μAcm^2 in different zones of the tested beams, supplied by galvanostats through counter electrodes made with stainless steel nets (50 cm long and the same width as the beam) located on the upper surface of the beams (Fig. 1).

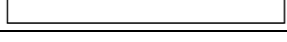
These zones of beams were moistened with a Sodium Chloride solution (0.3% by weight) and covered with an acrylic sheet (Fig. 2), in order to reduce evaporation and to secure a constant humidity. This electrolytic environment was obtained in the concrete around the reinforcements. The test period varied between 76 and 87 days.

In order to have evidence of bond loss, a beam area was selected where reinforcement bar corrosion process was accelerated, which length was equal to 25% of the total length of the beam (50 cm). Different locations for the affected area were selected to analyse the mechanical effects produced in each case (Table 1).

These beams were originally built to make standard bond tests, for this reason they had four bars, located at two levels. Only those from the upper face were affected by corrosion.

The penetration of the tendons was measured (according to the standard methodology UNE 7-436-82 in both ends of the beams that were subjected to accelerated corrosion. It

Table 1 Location of the corroded area and C/d adopted for each beam

Beam	Configuration	C/d
I		3.5
III		3.5
IV		3.5
V		3.5
XIV		3.5

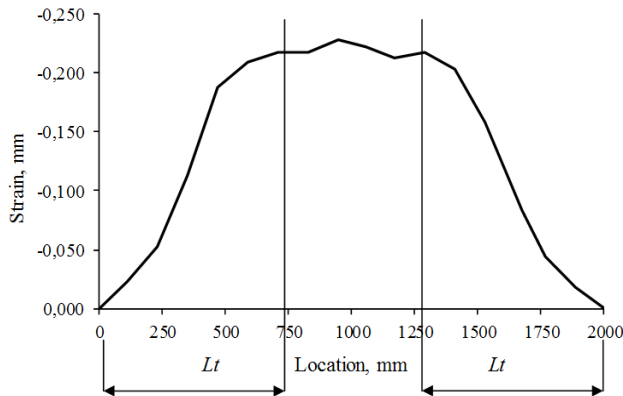


Fig. 3 Measured concrete strains in Beam 4, 7 days after loosening the tendons

was also studied cracking evolution; results are published in Ortega *et al.* (2001a), Ortega *et al.* (2001b).

2.4 Bond between concrete and prestressed rebars

This topic has been studied by several authors (Permanent Committee of the Concrete 1998, Leonhart 1988, Euro-International Committee of Concrete 1990, UNE 7-436-82 1993, European Committee of Normalization 1993, 1994). It is worth to mention that similar formulas are presented which enable to determine bond based on transfer length. This is the needed length to transmit the prestressed strength applied to the bars, to the concrete.

Fig. 3 shows the strain measured on the sides of one of the beams, as a function of the position inside the beam. The length where these strains vary is known as transfer length (L_t). It is worth to mention that in the reviewed bibliography a difference is made between transfer length and anchoring length (Permanent Committee of the Concrete 1998). The latter is necessary to ensure the strength of the anchorage by bond until steel failure occurs. It can be considered as a small increment of the former. For this reason, it was decided to work with the transfer length. In order to show this similarity, an example is presented: consider a structure with a 5% prestressing loss and under the conditions of the problem being studied, anchoring length is 7% bigger than transfer length. If prestressed losses were of 2%, this difference among both longitudes would be of 3%.

To determine transfer length (L_t), comments made by the

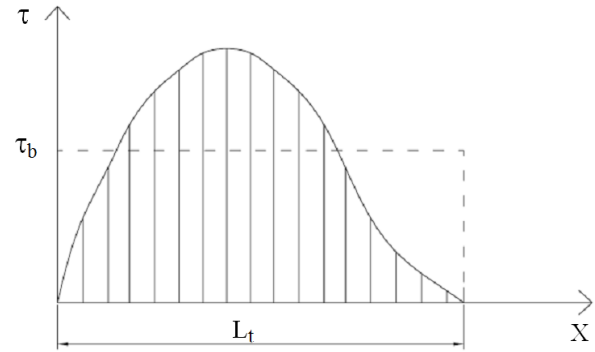


Fig. 4 Bond stress variation

Permanent Committee of the Concrete (1998) were employed, and it was determined as follows

$$L_t = \frac{\alpha_1 \times \alpha_2 \times \alpha_3 \times d \times \sigma_s}{4 \times \tau_b} \quad (1)$$

where:

$\alpha_1, \alpha_2, \alpha_3$ = series of coefficients that take into account: the way of introducing prestressing, the analyzed limit status and prestressed rebar type, which product was set at 0.7;

d = tendon nominal diameter;

σ_s = stress applied to the tendon at prestressing moment; and

τ_b = medium bond stress of prestressing, which is the average stress along of L_t (Fig. 4) and it is directly related to the reinforcement type (tendons or wires) and concrete strength.

Fig. 4 displays bond stress variation between the tendon and the concrete that for calculation purposes is adopted as constant. In this figure, it is considered that the beam free edge is located at $x=0$.

In the manufacture of prestressed beams, the tendons are put under tension and then precede the cast in place the concrete of the beam, when the concrete gets the design resistance, the ends of the prestressed bars are released, and these shorten trying to return to the original length (free of tensions), but the hardened concrete prevents it, leaving the beam with compression stress. Due to deformation and microcracking of the concrete that confines the tendons (zone located at the ends of the beam and known as transfer length), they penetrate into the mass of the concrete. This microcracking is in inverse relationship with the adhesion between steel and concrete, so that for a higher quality concrete there is less microcracking and therefore, greater adhesion.

Steel tendon and concrete bond calculation begins by measuring tendon penetration into the concrete (UNE 7-436-82 1993, LCPC 1999). The corrosion of reinforcement generates oxides on its external surface of them, it causes pressures on the cover that overcoming the tensile strength of concrete and cause cover cracks (parallel to the tendon), which do away with confinement of tendon, losing concrete-steel bond. As a result of this loss of bond, the tendon penetrates more easily into the mass of concrete. In order to quantify bond losses, as the corrosion process advances, the same testing technique is be used than to

Table 2 Average penetrations and transfer lengths determined by Eq. (4)

Tendons	Penetration (mm)	Transfer lengths (mm)	Average transfer length (mm)
Upper	2.227	633	527
Lower	1.480	421	

determine the bond between the tendons and the concrete. For these reasons, it should be related the penetration of the tendon end, to the transfer longitude. The increment of the strains along the transfer longitude is considered lineal, such as the one presented for the beam in Fig. 3. Considering the relationship between stress and strains (Hook's law), if the steel tendon strain (inside the concrete) is equalled to the penetration of the end of the bar, it is obtained

$$\frac{\delta}{L_t} = 0.5 \times \frac{\sigma_s}{E_s} \quad (2)$$

where:

δ = average penetration of the beam tendons
 E_s = Elasticity modulus of tendons steel

According to the norm followed during the test, it can be applied to the tendons, a stress equivalent to the 80 or 85 % of the ultimate strength (LCPC 1999) or the Steel Elastic Limit at 0.2% (UNE 7-436-82 1993), obtaining very similar load values. In this case, 80% of the ultimate strength was applied

$$\frac{\delta}{L_t} = 0.4 \times \frac{\sigma_m}{E_s} \quad (3)$$

where:

σ_m = tendon maximum stress (ultimate strength or Steel Elastic Limit at 0.2 %)

The transfer longitude remain as

$$L_t = 2.5 \times \frac{E_s}{\sigma_m} \times \delta \quad (4)$$

The coefficient 2.5 presented in the equation (4) differs from the one adopted by the UNE 7-436-82 (1993), which uses a coefficient of 3.5. For this reason, when this norm is followed the obtained longitudes are greater than the ones obtained when equation (4) is applied. On the other hand, the French norm LCPC (1999) uses a similar equation to find the anchorage longitude with a coefficient of 2.8.

Considering the test conditions ($E_s=215.800 \text{ Nmm}^{-2}$, $\sigma_m=1897 \text{ Nmm}^{-2}$), and replacing these parameters in the Eq. (4), the following is obtained

$$L_t(\text{mm}) = 284.4 \times \delta (\text{mm}) \quad (5)$$

Table 2 shows the average penetration of the upper and lower tendons, obtained in 10 beams, using all the measurements that were considered reliable.

It is worth to mention that the difference between the penetrations of the upper and lower tendons is because the bond in the upper part of the test specimens is smaller, as a result of concrete segregation (higher water/cement ratio).

This phenomenon is also noticed in reinforced concrete structures (Calavera Ruiz 2008).

Transfer lengths determined from the measured strains of the external beam faces of the test specimens considered in Table 2, presented an average of 65 cm after 7 days, according to norms (UNE 7-436-82 1993, LCPC 1999). Nevertheless, if the measurements are repeated after 14 days, the bond stress increases since the transfer lengths decrease a 15% approximately. In this case, the average transfer length is 55 cm, similar to the value obtained using Eq. (4), while the tendons penetrations practically did not change. The reason for this difference is that the transfer of efforts was not completed in 7 days. The connection curve between the constant strain zone and the effort transfer (L_t), shortens substantially.

This way, if the comparison of results is done after 14 days, the obtained values from the Eq. (4) are similar to those obtained following the french norm LCPC (1999). This norm finds the anchorage length which is always bigger than the transfer length (the difference depends on the prestressing losses), it can be stated both results match. These calculations are smaller than the $L_t=72 \text{ cm}$ that would be obtained following the norm UNE 7-436-82 (1993), which can be considered quite conservative.

Equaling the Eqs. (1) and (4) and calculating the bond stress

$$\tau_b (N/mm^2) = \left(0.056 \times d \times \frac{\sigma_m^2}{E_s} \right) \times \frac{1}{\delta} \quad (6)$$

it is obtained for the conditions outlined in this work

$$\tau_b (N/mm^2) = \frac{4.67 (Mmm^{-1})}{\delta (mm)} \quad (7)$$

3. Results

In Table 3 presents an overview of the results obtained in the test series. The second and the third column display the values of the registered penetrations from the introduction of the prestressed force (initial) and the measurements taken after the corrosion process was concluded (final). These penetrations enable to determine, by applying Eq. (5), the initial and final average bond stress of the corrosion process and then, by subtraction, bond losses are determined.

In order to establish the admissible bond stress which is used to do the calculations for the prestressed structures, the

Table 3 Summary of obtained results

Beam	Penetrations (mm)		Bond Stress (Nmm-2)		Bond Losses	
	Initial	Final	Initial	Final	Nmm-2	%
I	1.46	1.49	3.20	3.13	0.07	2.2
III	1.48	1.73	3.16	2.70	0.46	14.6
IV	2.09	3.44	2.23	1.36	0.87	39.0
V	1.41	1.46	3.31	3.20	0.11	3.3
XIV	1.50	1.61	3.11	2.90	0.21	6.8

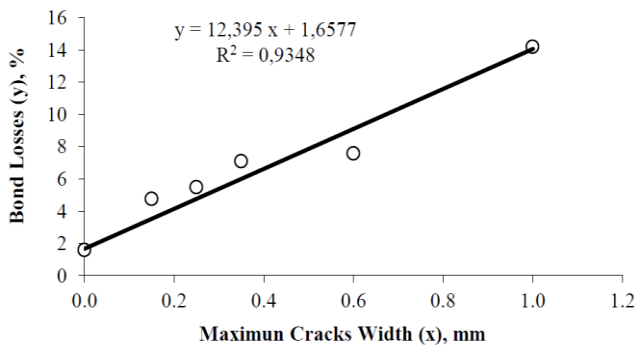


Fig. 5 Bond losses in accordance to maximum cracks width in Beam III

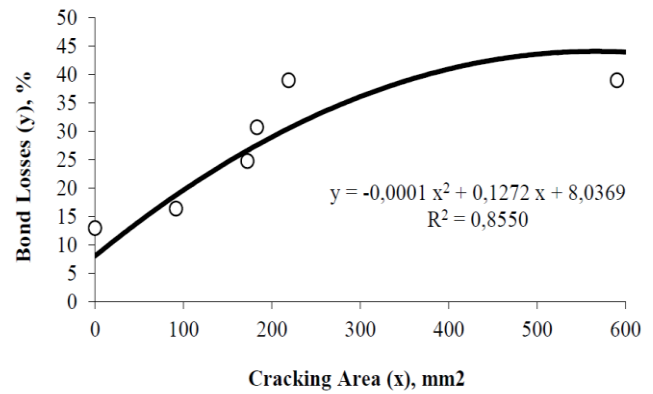


Fig. 8 Bond losses in accordance to maximum cracks width in Beam IV

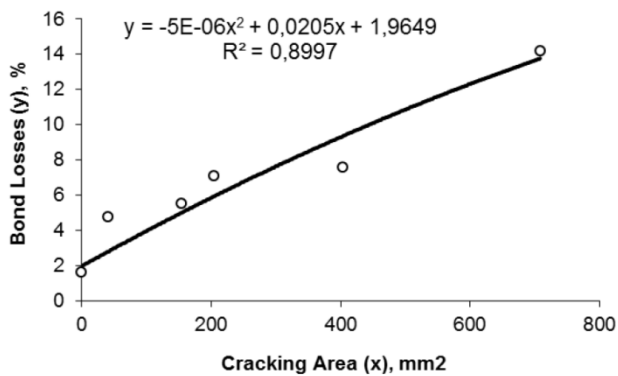


Fig. 6 Bond losses in accordance to cracking area in Beam III

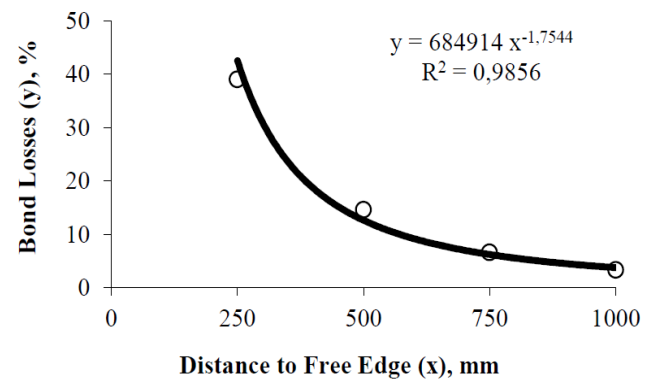


Fig. 9 Bond losses in accordance to maximum cracks width in Beam IV

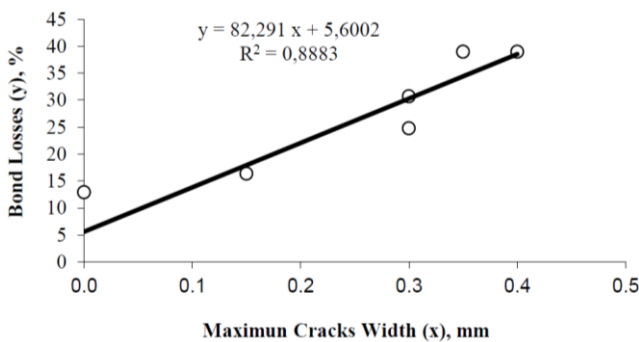


Fig. 7 Bond losses in accordance to maximum cracks width in Beam IV

initial bond stress should be divided (Table 3), by a safe coefficient which value depends on the followed norm, but usually, it is close to 2. In this way, for most of the beams, similar admissible bond stress values would be obtained to those included in the recommendations of Instruction of Structural Concrete.

Figs. 5 to 8 presents the evolution of these processes. Figs. 5 and 7 shows how bond losses increase in accordance with the maximum crack width. Figs. 7 and 9 represent bond losses on the “y” axis and cracking area on the “x” axis. This last parameter was considered more representative than their maximum width, due to the fact the latter only gives an idea of maximum degradation, while cracking area is related directly to the general condition of the rebar surface and this is closely related to the bonding

degree between concrete and steel. In all the cases, cracks ran parallel to the affected tendons; most of them appear on the sides of the beam.

4. Discussion

In Table 2 and Fig. 9 can be seen that as the affected area is further away from the free edge of the beam, bond losses decrease as it was expected. However, Beam I is an exception to this behavior because of the corrosion process, which in this case was extended to 76 days and no cracks were developed. In this only case, corrosion products came out through concrete pore structure, instead of accumulating around the area close to the rebars and due to the volume increase of the corroded steel, cover cracking occurs which produces a reduction of the concrete-steel contact surface and the confinement of the rebars. These two effects produce a progressive bond loss that leads to a reduction in the rebar stressing. Therefore, the beneficial effect of prestressing the structure is lost.

For the Beam IV, the transfer length of the tendon efforts to the concrete, has a length of 60 cm (measure 14 days after introducing the efforts), hence most of this length is affected by corrosion, even though the maximum cracking width was 0.4 mm, less than a half of the value registered for Beam VII, which had its central area affected, cracking area is similar. All this indicates that for Beam IV,

the cracking area is more uniform along the affected area.

Comparing the bond losses of the Beam I to the Beam IV, the first one presents no cracking but the latter does and both have the same area affected by corrosion. It can be stated that the layer of oxides formed around the tendons, is the responsible for approximately 5% of the bond loss stress, when cover cracking is present and tendon confinement is lost, they are the responsible of the remaining 95%. Beyond the relativity of the previous percentages, since only two tests were performed, it can be established that cracking is the parameter that has more influence on bond loss between concrete and steel tendons.

For Beam IV, the losses of the bond stress rise to the 39%. By Faraday's Law (Meneses *et al.* 2016), it can be stated that corrosion depth would be 0.28 mm, which means that almost 11% of the tendon cross section would have been lost.

On the other hand, less than the 20% of the Transfer Length of Beam III central area is affected. Therefore, the registered losses (tendon penetration) are lower. In this case, cracks are wider because the cover detached as a result of the pressure exerted by corrosion volume increase. Its thickness (about 2 cm) and the compression acting at both ends of the detached area makes the detachment process easier than if the affected area is located at one of the beam ends.

For Beam IV, it is interesting to mention another effect that may influence the cracking process. The stressed rebar within the concrete mass has a slightly lower diameter than the end exceeding the edge and it is stress free. Due to this diameter difference, a wedge is developed at the beam border that favors bonding which generates a radial stress on the concrete. This is known as "Hoyer effect" (Leonhart 1988). When rebars located at the end of a beam are affected by a corrosion process, this wedge favors cracking, reducing rebar confinement and therefore favoring contact loss between concrete and steel

5. Conclusions

The relevance of this research lies in the quantification of bond losses in prestressed structures with corroded tendons, especially, if it is considered that equations have been established that enable to evaluate with a certain degree of approximation, bond losses versus maximum crack width or cracking area.

In prestressed structures, processes of tendon corrosion are more degrading under the same conditions (cover thickness, concrete quality, etc.), than if reinforcements are not subjected to stress. Due to, for example, the appearance of impurities in the steel, local corrosion may appear that could lead to the failure of the prestressed bar, but if the affected area is bigger, it is quite probable that the gradual reduction of the bearing capacity is due to bond loss before the failure of the affected rebar. Such a case occurred during the development of this work by the displacement of the affected rebars. Even though bond losses were close to 40%, depending on the case, they could have produced the structure to collapse.

It can be concluded that general tendon corrosion is a

problem to be taken into account when it occurs in the area near to the cable beginning (anchorage area). It does not represent a high risk when it occurs at the central area, at least regarding bond loss. In this area, the most important inconveniences are embrittlement of the affected material and the possibility of section bar reduction until strength is lost.

Acknowledgments

This research was fully developed in the Engineering Department, and supported by the Science and Technology Secretariat, Universidad Nacional del Sur, Comisión de Investigaciones Científicas de la Provincia de Buenos Aires and Consejo Nacional de Investigaciones Científicas y Tecnológicas, Argentina

References

- Aimin, X. and Shayan A. (2016), "Relationship between reinforcing bar corrosion and concrete cracking", *ACI Mater. J.*, **113**(1), 3-12.
- Aveldaño, R.R. and Ortega, N.F. (2013), "Behavior of concrete elements subjected to corrosion in their compressed or tensed reinforcement", *Constr. Build. Mater.*, **38**, 822-828.
- Bhargava, K., Ghosh, A.K., Mori, Y. and Ramanujam, S. (2006), "Model for cover cracking due to rebar corrosion in RC structures", *Eng. Struct.*, **28**(8), 1093-1109.
- Cabrera, O.A., Ortega, N.F., Schierloh, M.I. and Traversa, L.P. (2012), "Influencia del curado sobre la evolución de la corrosión en vigas de hormigón armado con diferentes agregados finos", *Revista de la Asociación Latinoamericana de Control de Calidad, Patología y Recuperación de la Construcción*, **2**(2), 74-85.
- Calavera Ruiz, J. (2008), *Proyecto y calculo de estructuras de hormigón*, Vol. 1, Second edition, Intemac Ediciones, Madrid.
- Castaldo, P., Palazzo, B. and Mariniello, A. (2017), "Effects of the axial force eccentricity on the time-variant structural reliability of ageing rc cross-sections subjected to chloride-induced corrosion", *Eng. Struct.*, **130**, 261-274.
- Chung, L., Cho, S.H., Kim, J.H.J. and Yi, S.T. (2004), "Correction factor suggestion for ACI development length provisions based on flexural testing of RC slabs with various levels of corroded reinforcing bars", *Eng. Struct.*, **26**(8), 1013-1026.
- Comisión Permanente del Hormigón (1998), *Instrucción de Hormigón Estructural (EHE)*, Ministerio de Fomento.
- Comité Europeo de Normalización (1993), *Eurocódigo 2: Proyecto de estructuras de hormigón*, AENOR, Madrid, parte 1-1, 94-96, (1994), y parte 1-3, 24-26.
- Euro-International Committee of Concrete-International Federation of Prestressed, *Code Model CEB-FIP 1990 for structural concrete* (1995), Engineers College of Roads, Channels and Ports, Spanish Edition, Concrete Spanish Group-CEB and Prestressed Spanish Technical Association.
- Gerengi, H., Kocak, Y., Jazdzewska, A. and Kurtay, M. (2017), "Corrosion behavior of concrete produced with diatomite and zeolite exposed to chlorides", *Comput. Concrete*, **19**(2), 161-169.
- Hosseini, S.A., Shabakhty, N. and Mahini, S.S. (2015), "Correlation between chloride-induced corrosion initiation and time to cover cracking in RC Structures", *Struct. Eng. Mech.*, **56**(2), 257-273.

- Jin, L., Zhang, R., Du, X. and Li, Y. (2015), "Investigation on the cracking behavior of concrete cover induced by corner located rebar corrosion", *Eng. Fail. Anal.*, **52**, 129-143,
- Laboratoire Central des Points et Chaussées (1999), Determination of the conventional length of anchorage for bond, LCPC, 45-56.
- Leonhart, F. (1988), Estructuras de hormigón armado, Tomo V: Hormigónpretensado, (2º edición en español) Ed. Ateneo, Buenos Aires.
- Liu, M., Cheng, X., Li, X., Hu, J., Pan, Y. and Jin, Z. (2016), "Indoor accelerated corrosion test and marine field test of corrosion-resistant low-alloy steel rebars", *Case Stud. Constr. Mater.*, **5**, 87-99.
- Lollini, F., Redaelli, E. and Bertolini, L. (2016), "Corrosion assessment of reinforced concrete elements of Torre Velasca in Milan", *Case Stud. Constr. Mater.*, **4**, 55-61.
- Meneses, R.S., Moro, J.M., Aveldaño, R.R. and Ortega, N.F. (2016), "Influencia del espesor del recubrimiento de elementos de hormigón armado expuestos a procesos de corrosión y sometidos a cargas externas", *Revista de la Asociación Latinoamericana de Control de Calidad, Patología y Recuperación de la Construcción*, **6**(2), 46-61.
- Ortega, N.F., Alonso, M.C., Andrade, M.C. and López, C.; "Análisis de la Fisuración Ocasionada por la Corrosión de las Armaduras Activas de Elementos Pretensados", *Coloquia 2001*, Madrid, 10.
- Ortega, N.F., López, C., Alonso, M.C. and Andrade, M.C.; "Mecánica estructural de elementos de hormigón, con armaduras activas adherentes sometidas a la corrosión", *14º Reunión de la Asociación Argentina de Tecnología del Hormigón*, Olavarría, Argentina, 7.
- Ortega, N.F., Rivas, E.I., Aveldaño, R.R. and Peralta, M.H. (2011), "Beams affected by corrosion. influence of reinforcement placement in the cracking", *Struct. Eng. Mech.*, **37**(2), 72-81.
- Sajedi, S. and Huang, Q. (2015), "Probabilistic prediction model for average bond strength at steel-concrete interface considering corrosion effect", *Eng. Struct.*, **99**, 120-131.
- Soylev, T.A. and François, R. (2003), "Quality of steel-concrete interface and corrosion of reinforcing steel", *Cement Concrete Res.*, **33**(9), 1407-1415.
- UNE 7-436-82, Norma sobre el Método de Ensayo para la Determinación de las características de adherencia de las armaduras de pretensado, Tomo 4 Siderurgia, AENOR, Madrid.
- Yalciner, H., Eren, O. and Sensoy, S. (2012), "An experimental study on the bond strength between reinforcement bars and concrete as a function of concrete cover, strength and corrosion level", *Cement Concrete Res.*, **42**(5), 643-655.
- Yuksel, I. (2015), "Rebar corrosion effects on structural behavior of buildings", *Struct. Eng. Mech.*, **54**(6), 1111-1133.
- Zhao, Y., Dong, J., Wu, Y. and Jin, W. (2016), "Corrosion-induced concrete cracking model considering corrosion product-filled paste at the concrete/steel interface", *Constr. Build. Mater.*, **116**, 273-280.
- σ_s : stress applied to the tendon at prestressing moment
- τ_b : medium bond stress of prestressing, which is the medium stress along of L_t
- C/d : concrete cover and tendon diameter ratio
- d : tendon nominal diameter
- E_s : Elasticity modulus of tendons steel
- L_t : transfer length

CC

Notations

- series of coefficients that take into account: the
- $\alpha_1, \alpha_2, \alpha_3$: way of introducing prestressing, the analyzed limit status and prestressed rebar type
- δ : average beam tendon penetration
- σ_m : maximum stress applied to the tendon (ultimate strength or Elastic Limit of steel at 0.2 %)